J. For. Res. (2023) 34:1659–1668
https://doi.org/10.1007/s11676-023-01623-4

ORIGINAL PAPER

Effects of site productivity on individual tree maximum basal area growth rates of *Eucalyptus pilularis* in subtropical Australia

P. W. West[1]

Received: 7 February 2023 / Accepted: 26 April 2023 / Published online: 6 June 2023
© The Author(s) 2023

Abstract Inventory data were available from 96 plots of even-aged, monoculture, tall-open forests of *Eucalyptus pilularis* Smith, aged 2–63 years, growing in sub-tropical regions along the east coast of Australia. A model was developed relating the maximum possible stem basal area growth rate of individual trees to their stem basal area. For any tree size, this maximum increased as site productivity increased. However, the size at which this maximum occurred decreased as productivity increased. Much research has shown that, at any stand age, trees of a particular stem basal area are taller on more productive sites than on less productive ones. Taller trees incur greater respiratory costs to ensure maintenance of the photosynthetic capacity of their canopies; this reduces their growth rates. It was concluded that trees with larger basal areas will have the maximum possible growth rate on a less productive site, whilst trees with smaller basal areas will have the maximum possible on a more productive site. The model developed may constitute the first stage of a complete individual tree growth model system to predict wood yields from these forests.

Keywords Growth model · Individual tree · Maximum growth rate · *Eucalyptus pilularis* · Physiological effects

The online version is available at http://www.springerlink.com

Corresponding editor: Yu Lei.

Supplementary Information The online version contains supplementary material available at https://doi.org/10.1007/s11676-023-01623-4.

✉ P. W. West
pwest@nor.com.au

[1] Forest Research Centre, Southern Cross University, Lismore, NSW 2480, Australia

Introduction

One approach to the development of models to predict growth rates of individual trees in forests is to first construct a model predicting the maximum possible growth rate (sometimes termed potential or optimum growth rate) that a tree might have in relation to its size at the time growth is occurring (Smith et al. 1992; Pretzsch and Biber 2010; Weiskittel et al. 2011; Pommerening et al. 2022). Terms are then added to the model to predict the reductions from this maximum that are a consequence of both the particular environmental circumstances of the site on which the tree is growing and the competition it faces from its neighbours for the resources it requires for growth (light, water and nutrients).

The present work used growth data obtained from inventory plots of *Eucalyptus pilularis* Smith growing in sub-tropical regions along the east coast of Australia. Native forests of this species occur as tall-open forests that are generally even-aged and are often monocultures. The species has been of major commercial importance for timber production for many years and is sometimes grown in plantations. West (2021) developed a model relating the overall maximum stem basal area growth rates of individual trees to their basal areas. An objective of the present study was to extend that model to determine how those growth rate maxima were affected by changes in the productivity of the site on which the forest was growing. A second objective was to then relate the effects of both tree size and site productivity on growth rates to known physiological behaviour.

The model developed here should prove a useful starting point for an individual tree basal area growth rate model to which the effects of inter-tree competition and probability of death can be added subsequently to render a complete model useful for forest management.

Data

Sources

The data used here had been collected by the New South Wales and Queensland government forest services during 1931–1989 from 96 inventory plots located between 26–29° S and 152–153° E; this is only part of the total area of natural occurrence of *E. pilularis* (Boland et al. 2006). It should be appreciated that these data do not represent a formal sample of these forests but were those data available immediately over the period they were being collated (1983–1991) by Mattay and West (1994).

The plots were selected to be in even-aged stands and were essentially monospecific, with only rare inclusions of individuals of other species. Forest ages ranged over 2–63 years at the time of measurement. Plots varied in area over 0.04–0.2 ha and were measured 3–28 times at intervals of 0.4–5 years. At each measurement of a plot, diameters at breast height (1.3 m) over bark of live trees were recorded and, often, the heights of at least a sample of trees. In the entire data set, the largest diameter was 80 cm and the tallest individual was 55 m.

For every tree that survived between plot measurements, its basal area growth rate was determined as its change in basal area divided by the length of the growth period. Where data have come from growth periods longer than several years, others have determined values of basal area growth rate that incorporate information about the trend of growth rate with age over the growth period concerned (McDill and Amateis 1993; Cao 2000; Cao et al. 2002; Yue et al. 2012). In the present study, 90% of the growth rates were determined from growth periods of three years or less; it was felt there would be little advantage from using these more complex methods here. A total of 1,042 growth periods were measured over the 96 plots, giving 35,876 individual tree basal area growth rates.

Where heights had been measured, stand dominant height (average height of the 50 largest diameter trees per ha in a plot) was determined. Based on the dominant height at an age closest to 20 years, site productivity of each plot was determined as a site index, being the predicted dominant height at an index age of 20 years; site indices were estimated using functions developed by West and Mattay (1993). Site indices in the data set ranged over 13–40 m.

Selecting growth rate maxima

Models that aim to predict maximum possible individual tree growth rates on a site assume that data are available for trees growing free of competition. Only if the trees are open grown, is it possible to be certain of this (Smith et al. 1992). Given broad-scale plot data such as available here, it is impossible to identify exactly which trees conform to this requirement. However, when data are available for thousands of growth rates, perhaps it may be assumed that there are at least a few individuals growing essentially under those circumstances. Most models of this type have been developed assuming this is the case.

Thus, the first step in model development was to reduce the available data to leave only those for trees which had high growth rates for their size and which it might be hoped were free growing. This has been done in other studies with different species around the world (Coomes and Allen 2007; Pretzsch and Biber 2010; Pommerening et al. 2011; Bošeľa et al. 2013; Pommerening and Särkkä 2013; Pommerening and Maleki 2014; Häbel et al. 2019; Tian et al. 2021) using quantile regression (Koenker and Hallock 2001; Cade and Noon 2003). Other methods are available to achieve equivalent results (Bi and Turvey 1997; Bi et al. 2000; Zhang et al. 2005; Tian et al. 2021). For this study, the method of Bi and Turvey (1997) was used, termed here the 'class maxima' method. Note that, incorrectly, it was termed quantile regression in West (2021, 2022). This method was considered appropriate for the present work because it uses data that include, unequivocally, the maximum growth rates observed for the tree sizes encountered in the data set.

To use the class maxima method, the data set of 35,876 growth rate observations was split into 10 subsets, each containing trees from plots within a particular site index range. In the entire data set, trees were spread somewhat unevenly in numbers across plots with different site indices. However, attempts were made to choose site index classes that were roughly equal in width and contained substantial numbers of individual tree growth rates. Table 1 shows these site index classes and the number of observations in each data subset. Each subset was then split into 50 equal sized basal area classes and the observation with the highest growth rate in each size class was selected. Occasionally there were size classes which contained no observations and were ignored. A total of 460 observations were selected by this process over the 10 data subsets.

Figure 1 shows a scatter plot of the stand stocking densities against stand basal areas for the 1,042 plot measurement periods in the full data set. Superimposed on that is a corresponding scatter plot for the 460 observations that made up the 10 class maxima data subsets of maximum tree growth rates; many of those observations came from the same growth periods of the same plots and so share the same data point. The results suggest that the class maxima data tended to come from stands with lower stand basal areas and stocking densities, circumstances that are the most likely to include data for trees that are suffering little or no reductions in growth rates due to competition, as discussed previously. Note also, that quantification of the effects of inter-tree competition in these forests (West 2022) suggested

Table 1 Details of the 10 class maxima data subsets into which the data from 35,876 individual trees were split

Site index range in class subset (m)	Number of individuals in subset	Average site index of selected plots (m)	Parameter estimates, Model (1)		
			α	β	γ
31–40	2510	33.4	0.0223	0.0643	0.0419
30–31	2516	30.3	0.0600	0.4299	0.0791
28.5–30	10,609	28.9	0.0235	0.1447	0.0326
26–28.5	10,349	27.5	0.0273	0.1774	0.0495
25–26	2419	25.8	0.0610	0.3938	0.1398
23–25	1718	23.5	0.0305	0.2934	0.0606
22–23	1216	22.4	0.0159	0.0828	0.0222
20–22	1291	21.5	0.0326	0.3076	0.0743
17–20	1520	18.7	0.1042	0.7028	0.1324
13–17	1728	16.7	0.0164	0.3119	0.0237

The plot site index ranges used to split the data into each subset are shown, together with the number of trees in each subset. The average site index is shown of the plots from which came the 50 (at most) fastest growing individuals chosen from 50 equal sized basal area classes in each site index class. The parameter estimates determined for Model (1) in each site index class are shown

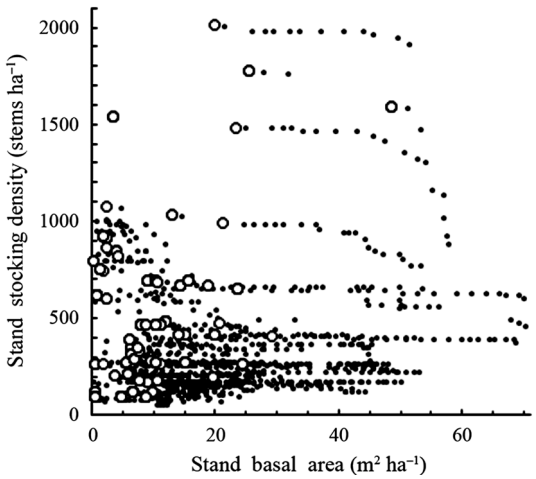


Fig. 1 Scatter plot of stand stocking densities against stand basal areas at the start of each of the 1,042 measurement periods of the 96 plots (●), together with data from the 460 observations from plots that contained trees with maximum growth rates and that were included in the 10 class maxima data subsets (○)

there are indeed instances where trees were growing free, or virtually so, of competition from their neighbours.

Scatter plots in Fig. 2 show the basal area growth rates against basal areas of individual tree data selected by this process for four of these class maxima data subsets; these four were chosen as examples to reflect the overall range of plot site indices in the whole data set. It was assumed that these growth rates in each subset were from trees growing with little competition from other trees and thus reflected the maximum growth rate possible for a tree of its size on a site with a productivity within the site index range used for each class. The supplementary material (Fig. S1) with this paper includes these scatter plots for all 10 class maxima data subsets.

Modelling

Model development

Model development was a two-stage process. The first stage involved the selection of a model function that would describe the selected class maxima data in any one of the 10 data subsets. The well-known Chapman-Richards function seemed suitable for this purpose (Pienaar and Turnbull 1973; Smith et al. 1992; Zeide 1993; West 2021) (Eq. 1):

$$\Delta B = \alpha B^{\beta} - \gamma B \quad (1)$$

where ΔB ($m^2\ a^{-1}$) is the basal area growth rate of an individual tree with basal area B (m^2), at the start of the growth period concerned, and α, β and γ are parameters. The non-linear Model (1) was fitted to the data of each of the 10 data subsets by least-squares regression using the NLIN procedure of the SAS statistical package.[1] The parameter estimates for each data subset are shown in Table 1; the fit to the data of this model for each example data set is shown in Fig. 2.

A second-stage model was then developed to attempt to determine how site productivity, as estimated by stand site index, affected tree growth rates. Scatter plots were drawn of the first-stage parameter estimates against the average site index (S, m) of the plots from which the data had been

[1] Documentation for the SAS statistical package is available at https://support.sas.com/en/documentation.html (accessed May 2023).

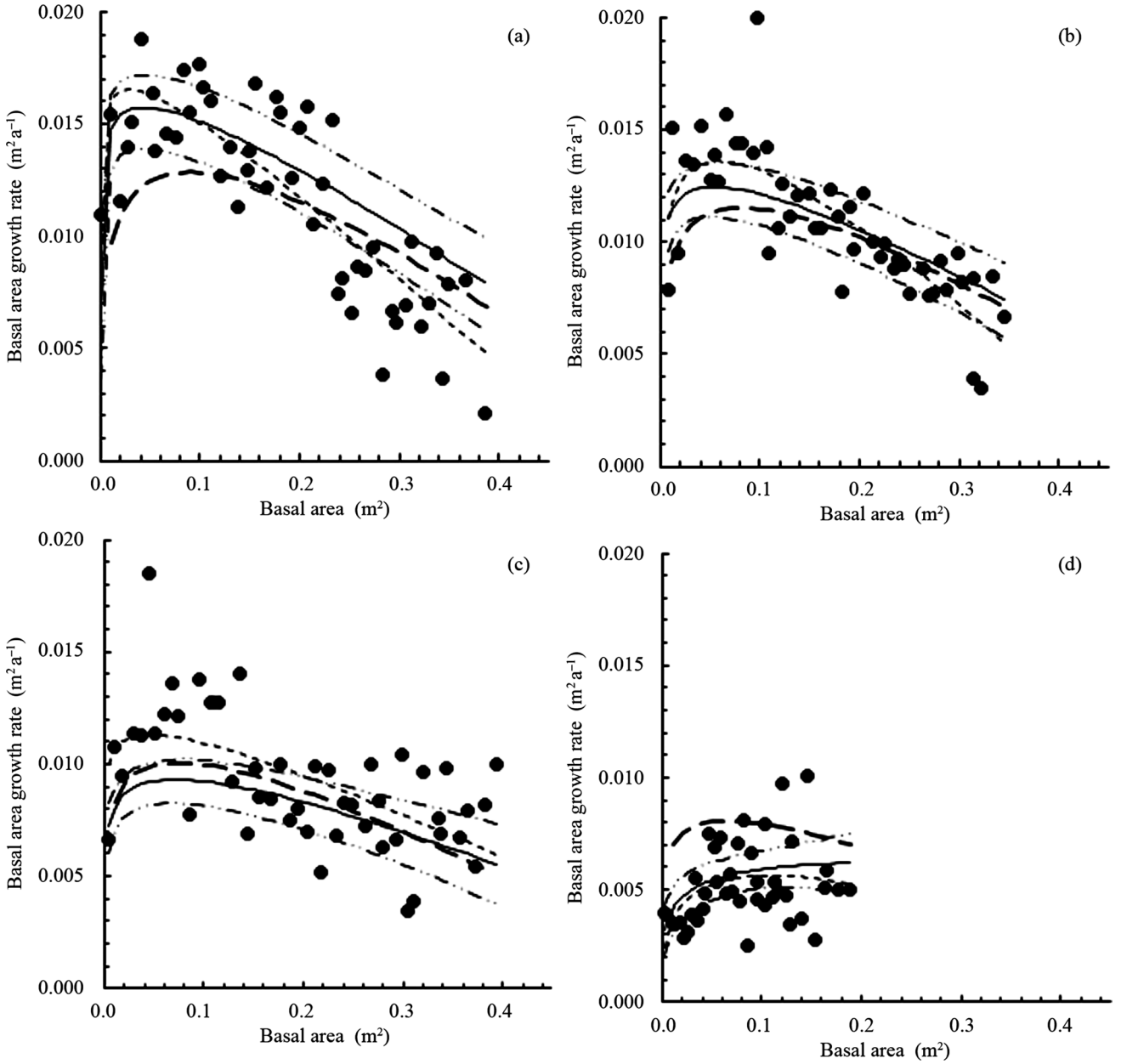


Fig. 2 Scatter plots (•) of individual tree basal area growth rates against tree basal areas, at the start of the growth period concerned, of the data included in four examples of the class maxima data sets constructed here from plots with site indices in the ranges **a**: 31–40 m, **b**: 26–28.5 m, **c**: 22–23 m and **d**: 13–17 m. The short, dashed lines (- - - -) show the fit to the data in each case of the first-stage Model (1), fitted with nonlinear regression, with parameter estimates as in Table 1. The solid lines (————) show the fit to the data of the model incorporating site index Model (3), for which the parameter estimates are in Table 2 using data pooled over all 10 class maxima data subsets. The lines (– .. – .. –) show the upper and lower 95% confidence limits about estimates of basal area growth rate from this model. The long, dashed lines (– – –) show the fit to the data of the Model (2) of West (2022)

included in each data subset (Table 1). Examination of these scatter plots suggested that, of the three parameters, the value of the parameter β was the one most closely related to stand site index. The scatter plot of those data is shown in Fig. 3a. It appeared that the model

$$\beta = \exp\left[\beta_1 + \beta_2 \ln\left(\overline{S}\right)\right] \tag{2a}$$

could be used to describe the relationship, albeit rather poorly; the ordinary least-squares straight line fit of the

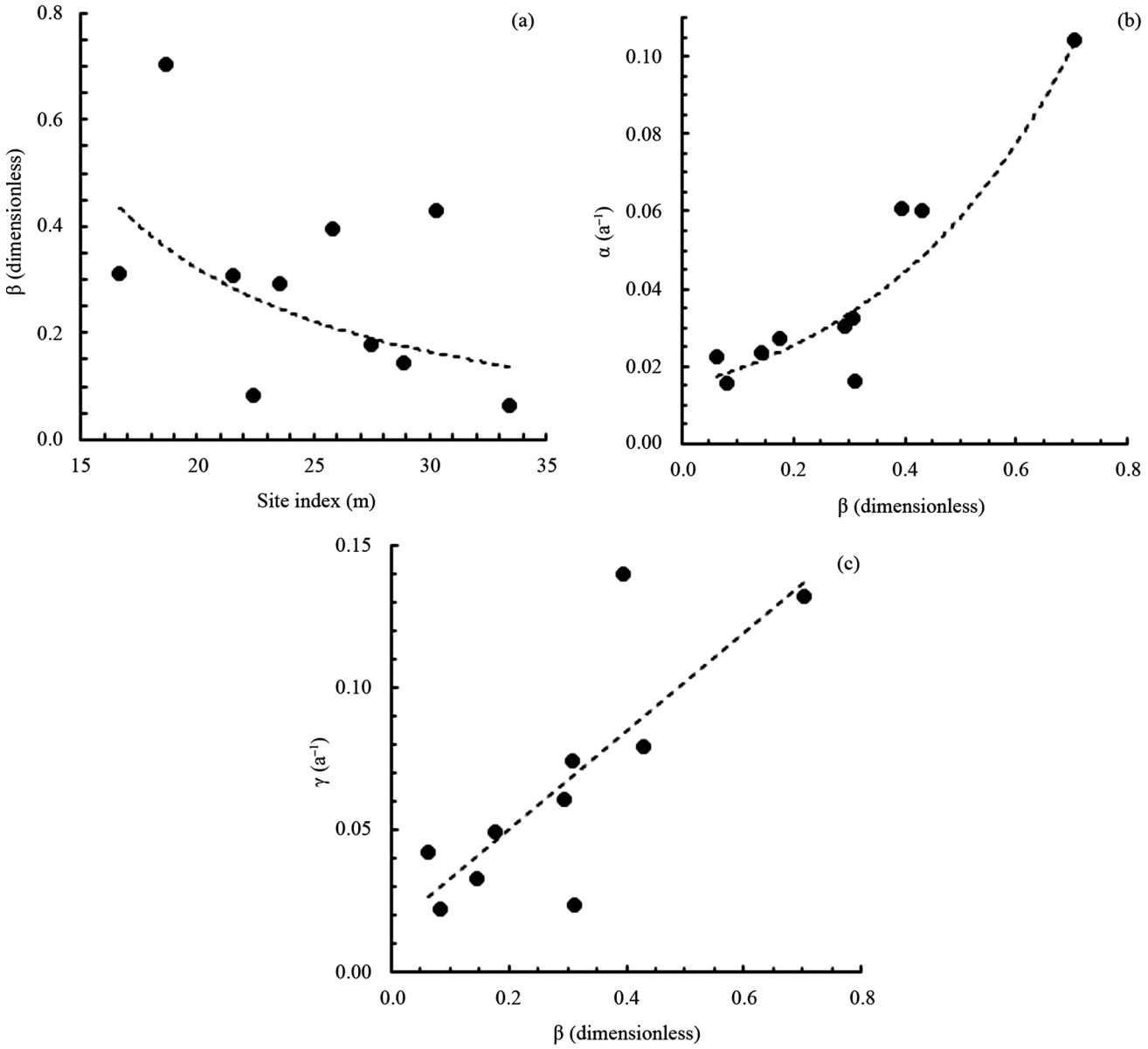


Fig. 3 Scatter plots (●) of the relationships between the parameter estimates of Model (1) (Table 1) and the variable with which each appeared to be most closely related. The lines show the ordinary least-squares fit to the data of **a**: Model (2a), **b**: Model (2b) and **c**: Model (2c)

data, using the logarithmic expression of Model (2a), had an r^2 value of only 21%. It was then recognised that both parameters α and γ were related closely to β over the 10 data subsets; the corresponding scatter plots are shown in Figs. 3b and 3c. It then appeared that appropriate second-stage models for those two parameters might be:

$$\alpha = \alpha_1 \exp(\alpha_2 \beta) \tag{2b}$$

and

$$\gamma = \gamma_1 + \gamma_2 \beta \tag{2c}$$

Equation 2a was substituted into each of Eqs. 2b and 2c and the results then substituted into Eq. 1. This yielded a rather complex, nonlinear model involving the six parameters α_1, α_2, β_1, β_2, γ_1 and γ_2, where each of β_1 and β_2 appeared three times at different positions in the model. This model may be written more fully as:

$$\Delta B = \alpha_1 \exp\left[\alpha_2 f\left(\beta, \overline{S}\right)\right] B^{f\left(\beta, \overline{S}\right)} - \left[\gamma_1 + \gamma_2 f\left(\beta, \overline{S}\right)\right] B \tag{3}$$

where

Table 2 Parameter estimates of Model (3) and their standard errors

Parameter	Estimate	Standard error
α_1	0.043	0.018
α_2	−7.599	4.346
β_1	1.566	1.183
β_2	−1.147	0.363
γ_1	0.055	0.015
γ_2	−0.256	0.142

$$f\left(\beta,\bar{S}\right)=\exp\left[\beta_1+\beta_2\ln\left(\bar{S}\right)\right]$$

The NLIN procedure of the SAS package readily fitted this complex model to the 460 observations pooled over the 10 class maxima data subsets. The parameter estimates with their standard errors are shown in Table 2.

A potential problem with fitting a model to this pooled data set was that, whilst there may be random variation in the observed data of any one data subset for any one site index class, its average behaviour might differ from that of other data subsets of the same class that might have occurred, by chance, in the data. Under these circumstances, the residuals from the fitted model in any one data subset may no longer be independent of each other, a principal requirement of least-squares regression analysis. This correlation (covariance) between the residuals within a data subset may not lead to bias in the parameter estimates obtained for the model, but it must be accounted for if their standard errors are to be estimated without bias. This is the same problem as encountered in data sets that contain multiple measurements within individual sampling units (Cole and Grizzle 1966; Dielman 1983; West et al. 1984; Fitzmaurice et al. 2011). As West and Ratkowsky (2022) noted, various solutions to this problem have been suggested but not all are applicable with nonlinear models or can be relied upon on under all circumstances.

In the present case, Model (3) appeared to fit the data reasonably well. The fit in each of the four example data subsets is shown as the solid lines in Fig. 2. Inevitably, since such fitted lines represent predictions made using the average site index of the plots that made up the data in each subset, there appear to be some deviations from the fit to the data for each of the example data sets (the solid lines). However, scatter plots of the residuals against the fitted values from Model (3) did not show any marked pattern nor any tendency of a positive or negative bias in any subset. This suggested that the estimate of the covariance matrix of the parameter estimates was unlikely to have any substantial bias. The corresponding 95% confidence limits about estimates of basal area growth rates using the pooled model are shown as the more complex dashed lines in each of the examples in Fig. 2. These confidence limits were determined using the method of Box (1971), as shown in Eq. 9.6 of Ratkowsky (1983), and the estimate of the covariance matrix of the parameter estimates provided by the NLIN procedure of the SAS package. The fit to the data of Model (3) for all 10 class maxima data subsets is shown in the Supplementary material.

As an alternative to this use of nonlinear regression to fit Model (3), it is perhaps inviting to fit the set of Models (2a–c) jointly using the 3SLS method of seemingly unrelated regression (SUR) (Zellner 1962, 1963; Srivastava and Giles 1987). It was found that whilst this method gave an adequate fit to the data, it grossly overestimated the confidence limits about the fitted lines. This was probably a consequence of having only 10 observations to fit the model with SUR, whereas the nonlinear regression (Model 3) was based on 460 observations.

An earlier model relating maximum tree basal area growth rates to tree basal areas and site productivity was developed by West (2022) using largely the same inventory data. The fit to the data of that model is shown in Fig. 2 with long dashed lines. It fitted the data well for stands with mid-level site indices (Fig. 2b and c), but underestimated growth rates in stands with higher site indices (Fig. 2a) and over-estimated in stands with lower site indices (Fig. 2d). That model was less complex in form than the present model and this probably led to its somewhat poorer fit to the data.

Application of model

Figure 4 shows predictions from Model (3) of individual tree maximum basal area growth rates in relation to basal areas for each of a set of five site indices. It shows clearly how maximum growth rate for trees of any basal area increased with increasing site index, consistent with the trends in the data for the four site index classes in Fig. 2.

Within any one stand, the model predicts that maximum growth rate increases progressively with tree size, to an overall maximum for the stand and then declines progressively as tree size increases further. This is the form predicted by the Chapman-Richards function (Model 1). With straightforward calculus, it is easy to show that the basal area (B_m, m^2), at which that overall maximum occurs in any stand, may be predicted as:

$$B_m=\left[\gamma/(\alpha\beta)\right]^{\left[1/(\beta-1)\right]} \quad (4)$$

For a stand of any site index S(m), Models (2a–c) may be used to give values for α, β and γ for use in Eq. 4.This was used in drawing the dashed line in Fig. 4. The corresponding overall maximum growth rate for that site index may then be determined by applying B_m for B in Model (1).

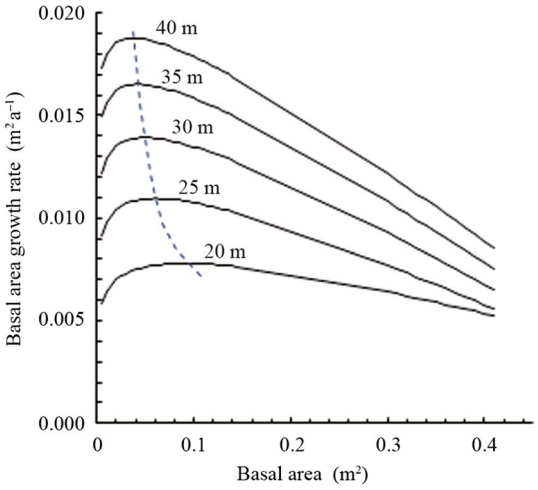


Fig. 4 Predictions (——) for five stands, with site indices as indicated, of maximum basal area growth rates from Model (3) using the parameter estimates in Table 2. The line (- - - -) shows how, in any stand, the basal area of the tree that shows the greatest growth rate of all trees in that stand tends to decline with increasing site productivity

The dashed line (Fig. 4) shows how B_m tends to increase progressively as stand site productivity declines. Over the site index range 20–40 m, the progressive increase in B_m corresponds to a progressive increase in stem diameters over the range 22–34 cm. The corresponding overall maximum growth rate declines progressively as stand site productivity declines.

Discussion and conclusions

As discussed in earlier work (West 2021, 2022), the Chapman-Richards function as displayed here is consistent with the well-known phenomenon that stand growth rates of even-aged forests increase during their early years, but within a few decades, reach a maximum and decline progressively thereafter. Various reviews and texts describe this phenomenon (Gower et al. 1996; Ryan et al. 1997; Davis et al. 2001; West 2015; Binkley 2023). These trends are evident in whatever measures of tree size are used, measures such as biomass, wood volume or characteristics correlated with these, such as stem basal area. During early stand development, individual tree growth rates increase with size, hence age. Stand growth is the sum of individual tree growths, so as trees become larger, stand growth rate will become correspondingly bigger. However, after some years, some trees will reach a size at which their growth rates decline, consistent with the trends in maximum possible growth rates shown in Figs. 2 and 4. Over time, more and more trees will reach this size and stand growth rates will continue to decline, the decline increasing steadily with increasing tree size, that is, with increasing stand age.

Since the mid-twentieth century, forest research has sought to explain this growth behaviour. Consideration of various alternatives led Binkley (2023) to conclude that the most likely cause was a reduction with age (hence size) of the 'efficiency' of tree growth, i.e., the amount of growth per unit of light, water and nutrients that a tree obtains from the environment. A theory consistent with this, which has received considerable support, is the 'hydraulic limitation theory'. This proposed that water stress in leaves increases as taller trees must transport water from roots to leaves to greater heights; this was assumed to reduce the photosynthetic capability of their canopies (Ryan et al. 1997, 2006; Koch et al. 2004), that is, reducing their growth efficiency with respect to the amount of light their crowns intercepted. More recently, it has been suggested that the decline in efficiency is due to respiratory costs increasing progressively with tree size (West 2020). In this theory, it is suggested that greater respiratory costs are incurred in processes such as construction of more complex anatomy of newly developing leaves, changes that ameliorate photosynthetic limitations of the canopy due to water stress.

These physiological phenomena may provide an answer to the objective of this study to explain how varying site productivities affect individual tree maximum stem growth rates (Fig. 4). Several studies, with different tree species in various parts of the world, have developed models relating tree height to stem diameter across tree populations (Curtis 1967; Krumland and Wensel 1988; Hanus et al. 1999; Calama and Montero 2004; Dorado et al. 2006; Crecente-Campo et al. 2010; Gómez-García et al. 2014; Sharma et al. 2016; Zhang et al. 2019; Raptis et al. 2021; Lin et al. 2022). They have found that trees of the same diameter are taller in stands with greater dominant heights (defined as the average height of a restricted number of the tallest or largest diameter trees in a stand). However, heights and diameters will increase progressively with age. Consider two stands of the same age but growing on sites of different productivity. The dominant height on the more productive site will be greater than that on the less productive site. This is the principle on which is based the concept of using site index (dominant height of trees at an arbitrarily chosen age, West 2015) as a measure of site productivity. Trees of the same diameter on the two sites will then be taller on the more productive site and hence, more likely to show a decline in growth rate in consequence of the physiological constraints they are suffering. Thus, it will be trees of larger diameters beyond which maximum growth rates will start to decline on the less productive site.

Teck and Hilt (1991) developed functions to relate maximum individual stem growth rates to stem size and stand site index and used growth data collected from many forest plots over periods of many years. They used data from 28 softwood

and hardwood species that occur in forests across northeastern USA. Similar work by Pretzsch and Biber (2010) considered two softwood and two hardwood species from forests of Bavaria, Germany. The function used by Teck and Hilt was:

$$\Delta B = aS\left[1 - \exp(-bD)\right] \quad (5)$$

whilst Pretzsch and Biber used:

$$\Delta D = (a + bS)D^{c}\exp(-dD) \quad (6)$$

where, ΔB is individual tree basal area growth rate, ΔD is diameter growth rate, D is stem diameter at the start of a growth period, S is stand site index and a, b, c and d are parameters. In both cases, the functions they fitted predicted that the overall maximum growth rate increased with increasing site index, as was case in the present study. However, Eq. 5 simply predicts maximum basal area growth rate to increase with tree size and does not predict that it will reach some overall maximum at a specific basal area. Equation 6 does allow for the determination of a size at which maximum growth rate is an overall maximum, but that size is the same for any site index. Neither of these models yielded results similar to those of Fig. 4, results that appear to show a behaviour consistent with the known physiological behaviour of tall trees.

Model (3) developed here may be used as the first stage of a more general model to predict individual basal area growth rates in relation to tree size in *E. pilularis* forest in its natural range of sub-tropical eastern Australia. The next stage in the development of such a model would be to determine the reductions from the maximum possible growth rates due to the effects of inter-tree competition for growth resources where trees are growing sufficiently close to each other and to determine the likelihood of mortality (Belcher et al. 1982; Wensel et al. 1987; Teck and Hilt 1991; Lessard et al. 2001; Bragg 2001; Pretzsch and Biber 2010; West 2022). Further work would be required to extend the model to predict variables of interest to forest management such as tree height, biomass or wood volume. This would often use allometric relationships between these characteristics and stem diameter or basal area (West 1979, 1982, 2015; Paul et al. 2016).

Acknowledgements I am grateful to my colleague, Dr D.A. Ratkowsky, for valuable discussions related to methods to fit the model developed here. Journal reviewers offered a number of useful suggestions to improve the manuscript.

Funding Open Access funding enabled and organized by CAUL and its Member Institutions.

Open Access This article is licensed under a Creative Commons Attribution 4.0 International License, which permits use, sharing, adaptation, distribution and reproduction in any medium or format, as long as you give appropriate credit to the original author(s) and the source, provide a link to the Creative Commons licence, and indicate if changes were made. The images or other third party material in this article are included in the article's Creative Commons licence, unless indicated otherwise in a credit line to the material. If material is not included in the article's Creative Commons licence and your intended use is not permitted by statutory regulation or exceeds the permitted use, you will need to obtain permission directly from the copyright holder. To view a copy of this licence, visit http://creativecommons.org/licenses/by/4.0/.

References

Belcher DW, Holdaway MR, Brand GJ (1982) STEMS: The stand and tree evaluation modeling system. Gen. Tech. Rep. NC−79, USDA, Forest Service, North Central Forest Experiment Station, St Paul, MN

Bi HQ, Turvey ND (1997) A method of selecting data points for fitting the maximum biomass-density line for stands undergoing self-thinning. Aust J Ecol 22(3):356–359. https://doi.org/10.1111/j.1442-9993.1997.tb00683.x

Bi HQ, Wan G, Turvey ND (2000) Estimating the self-thinning boundary line as a density-dependent stochastic biomass frontier. Ecology 81(6):1477–1483. https://doi.org/10.1890/0012-9658(2000)081[1477:ETSTBL]2.0.CO;2

Binkley D (2023) Acorn review: the persistent mystery of declining growth in older forests. For Ecol Manag 538:121004. https://doi.org/10.1016/j.foreco.2023.121004

Boland DJ, Brooker MIH, Chippendale GM, Hall N, Hyland BPM, Johnston RD, Kleinig DA, Turner JD (2006) Forest trees of Australia, 5th edn. CSIRO, Canberra

Bošeľa M, Petráš R, Šebeň V, Mecko J, Marušák R (2013) Evaluating competitive interactions between trees in mixed forests in the Western Carpathians: comparison between long-term experiments and SIBYLA simulations. For Ecol Manag 310:577–588. https://doi.org/10.1016/j.foreco.2013.09.005

Box MJ (1971) Bias in nonlinear estimation. J R Stat Soc Ser B Methodol 33(2):171–201. https://doi.org/10.1111/j.2517-6161.1971.tb00871.x

Bragg DC (2001) Potential relative increment (PRI): a new method to empirically derive optimal tree diameter growth. Ecol Mod 137(1):77–92. https://doi.org/10.1016/S0304-3800(00)00433-6

Cade BS, Noon BR (2003) A gentle introduction to quantile regression for ecologists. Front Ecol Environ 1(8):412–420. https://doi.org/10.2307/3868138

Calama R, Montero G (2004) Interregional nonlinear height-diameter model with random coefficients for stone pine in Spain. Can J for Res 34(1):150–163. https://doi.org/10.1139/X03-199

Cao QV (2000) Prediction of annual diameter growth and survival for individual trees from periodic measurements. For Sci 46(1):127–131. https://doi.org/10.1093/forestscience/46.1.127

Cao QV, Li S, McDill ME (2002) Developing a system of annual tree growth equations for the loblolly pine shortleaf pine type in Louisiana. Can J for Res 32(11):2051–2059. https://doi.org/10.1139/x02-12

Cole JWL, Grizzle JE (1966) Applications of multivariate analysis of variance to repeated measurements experiments. Biometrics 22:810–828

Coomes DA, Allen RB (2007) Effects of size, competition and altitude on tree growth. J Ecol 95(5):1084–1097. https://doi.org/10.1111/j.1365-2745.2007.01280.x

Crecente-Campo F, Tomé M, Soares P, Diéguez-Aranda U (2010) A generalized nonlinear mixed-effects height-diameter model for *Eucalyptus gobulus* L. in northwestern Spain. For Ecol Manage 259(5):943–952. https://doi.org/10.1016/j.foreco.2009.11.036

Curtis RO (1967) Height–diameter and height–diameter-age equations for second-growth Douglas-Fir. For Sci 13(4):365–375. https://doi.org/10.1093/forestscience/13.4.365

Davis LS, Johnson KN, Bettinger PS, Howard TE (2001) Forest management, 4th edn. McGraw-Hill, New York

Dielman T (1983) Pooled cross-sectional area and time series data. A survey of current statistical methodology. Am Stat 37(2):111–122. https://doi.org/10.1080/00031305.1983.10482722

Dorado FC, Diéguez-Aranda U, Anta MB, Rodríguez MS, von Gadow K (2006) A generalized height-diameter model including random components for radiata pine plantations in northwestern Spain. For Ecol Manag 229(1–3):202–213. https://doi.org/10.1016/j.foreco.2006.04.028

Fitzmaurice GM, Laird NM, Ware JH (2011) Applied longitudinal analysis, 2nd edn. Wiley Inter-science, Hoboken

Gómez-García E, Diéguez-Aranda U, Castedo-Dorado F, Crecente-Campo F (2014) A comparison of model forms for the development of height-diameter relationships in even-aged stands. For Sci 60(3):560–568. https://doi.org/10.5849/forsci.12-099

Gower ST, McMurtrie RE, Murty D (1996) Aboveground net primary production decline with stand age: potential causes. Trends Ecol Evol 11(9):378–382. https://doi.org/10.1016/0169-5347(96)10042-2

Häbel H, Myllymäki M, Pommerening A (2019) New insights on the behaviour of alternative types of individual-based tree models for natural forests. Ecol Model 406:23–32. https://doi.org/10.1016/j.ecolmodel.2019.02.013

Hanus ML, Marshall DD, Hann DW (1999) Height-diameter equations for six species in the coastal regions of the Pacific Northwest. Res. Contribution 25, Forest Research Laboratory, Oregon State University, Corvallis

Koch GW, Sillett SC, Jennings GM, Davis SD (2004) The limits to tree height. Nature 428:851–854. https://doi.org/10.1038/nature02417

Koenker R, Hallock KF (2001) Quantile regression. J Econ Perspect 15(4):143–156. https://doi.org/10.1257/jep.15.4.143

Krumland BE, Wensel LC (1988) A generalized height-diameter equation for coastal Californian species. Western J Appl for 3:113–115

Lessard VC, McRoberts RE, Holdaway MR (2001) Diameter growth models using Minnesota forest inventory and analysis data. For Sci 47(3):301–310. https://doi.org/10.1093/forestscience/47.3.301

Lin FC, Xie LF, Hao YS, Miao Z, Dong LH (2022) Comparison of modeling approaches for the height-diameter relationship: an example with planted Mongolian pine (*Pinus sylvestris* var. *mongolica*) trees. Forests 13(8):1168. https://doi.org/10.3390/f13081168

Mattay JP, West PW (1994) A collection of growth and yield data from eight eucalypt species growing in even-aged monoculture forest. User Series No. 18, CSIRO Division of Forestry, Canberra

McDill ME, Amateis RL (1993) Fitting discrete-time dynamic models having any time interval. For Sci 39(3):499–519. https://doi.org/10.1093/forestscience/39.3.499

Paul K, Roxburgh SH, Chave J, England JR, Zerihun A, Specht A, Lewis T, Bennett LT, Baker TG, Adams MA, Huxtable D, Montagu KD, Falster DS, Feller M, Sochacki S, Ritson P, Bastin G, Bartle J, Wildy D, Hobbs T, Larmour J, Waterworth R, Stewart HTL, Jonson J, Forrester DI, Applegate G, Mendham D, Bradford M, O'Grady A, Green D, Sudmeyer R, Rance SJ, Turner J, Barton C, Wenk EH, Tim Grove PM, Attiwill EP, Butler D, Brooksbank K, Spencer B, Snowdon P, O'Brien N, Battaglia M, Cameron DM, Hamilton S, McAuthur G, Sinclair J (2016) Testing the generality of above-ground biomass allometry across plant functional types at the continent scale. Global Change Biol 22(6):2106–2124. https://doi.org/10.1111/gcb.13201

Pienaar LV, Turnbull KJ (1973) The Chapman-Richards generalization of von Bertalanffy's growth model for basal area growth and yield in even-aged stands. For Sci 19(1):2–22. https://doi.org/10.1093/forestscience/19.1.2

Pommerening A, Maleki K (2014) Differences between competition kernels and traditional size-ratio based competition indices used in forest ecology. For Ecol Manag 331:135–143. https://doi.org/10.1016/j.foreco.2014.07.028

Pommerening A, Särkkä A (2013) What mark variograms tell about spatial plant interactions. Ecol Model 251:64–72. https://doi.org/10.1016/j.ecolmodel.2012.12.009

Pommerening A, LeMay V, Stoyan D (2011) Model-based analysis of the influence of ecological processes on forest point pattern formation-a case study. Ecol Model 222(3):666–678. https://doi.org/10.1016/j.ecolmodel.2010.10.019

Pommerening A, Sterba H, West P (2022) Sampling theory inspires quantitative forest ecology: the story of the relascope kernel function. Ecol Model 467:109924. https://doi.org/10.1016/j.ecolmodel.2010.10.019

Pretzsch H, Biber P (2010) Size-symmetric versus size-asymmetric competition and growth partitioning among trees in forest stands along an ecological gradient in central Europe. Can J for Res 40(2):370–384. https://doi.org/10.1139/X09-195

Raptis DI, Kazana V, Onisiforou N, Stamatiou C, Kazaklis A (2021) Height allometry of *Pinus nigra* Arn. in Troodos National Forest Park, Cyprus. Sustainability 13(11):5998. https://doi.org/10.3390/su13115998

Ratkowsky DA (1983) Nonlinear regression modeling. Marcel Dekker, New York

Ryan MG, Binkley D, Fownes JH (1997) Age-related decline in forest productivity: pattern and process. Adv Ecol Res 27:213–262. https://doi.org/10.1016/S0065-2504(08)60009-4

Ryan MG, Phillips N, Bond BJ (2006) The hydraulic limitation hypothesis revisited. Plant Cell Environ 29(3):367–381. https://doi.org/10.1111/j.1365-3040.2005.01478.x

Sharma RP, Vacek Z, Vacek S (2016) Modeling individual tree height to diameter ratio for Norway spruce and European beech in Czech Republic. Trees 30(6):1969–1982. https://doi.org/10.1007/s00468-016-1425-2

Smith WR, Farrar RM, Murphy PA, Yeiser JL (1992) Crown and basal area relationships of open-grown southern pines for modeling competition and growth. Can J for Res 22(3):341–347. https://doi.org/10.1139/x92-044

Srivastava VK, Giles DEA (1987) Seemingly unrelated regression equations models. CRC Press, Boca Raton

Teck RM, Hilt DE (1991) Individual-tree diameter growth model for the northeastern States. Res. Paper NE−649, Northeast Forest Experiment Station, Radnor, Pa

Tian DC, Bi HQ, Jin XJ, Li FR (2021) Stochastic frontiers or regression quantiles for estimating the self-thinning surface in higher dimensions? J for Res 32:1515–1533. https://doi.org/10.1007/S11676-020-01196-6

Weiskittel AR, Hann DW, Kershaw JA, Vanclay JK (2011) Forest growth and yield modelling. Wiley-Blackwell, Oxford

Wensel LC, Meerschaert WJ, Biging GS (1987) Tree height and diameter growth models for northern California conifers. Hilgardia 55:1–20

West PW (1979) Estimation of height, bark thickness and plot volume in regrowth eucalypt forest. Aust for Res 9(4):295–308

West PW (1982) Functions to estimate tree height and bark thickness of Tasmanian regrowth eucalypts. Aust for Res 12:183–190

West PW (2015) Tree and forest measurement, 3rd edn. Springer International Publishing, Switzerland

West PW (2020) Do increasing respiratory costs explain the decline with age in forest growth rate? J for Res 31(3):693–712. https://doi.org/10.1007/s11676-019-01020-w

West PW (2021) Modelling maximum stem basal area growth rates of individual trees of *Eucalyptus pilularis* Smith. For Sci 67(6):633–636. https://doi.org/10.1093/forsci/fxab047

West PW (2022) Quantifying effects on tree growth rates of symmetric and asymmetric inter-tree competition in even-aged, monoculture *Eucalyptus pilularis* forests. Trees 37:239–254. https://doi.org/10.1007/s00468-022-02341-w

West PW, Mattay J (1993) Yield prediction models and comparative growth rates for six eucalypt species. Aust for 56(3):211–225. https://doi.org/10.1080/00049158.1993.10674609

West PW, Ratkowsky DA (2022) Simulation studies comparing fixed effect and mixed models in data sets with multiple measurements in individual sampling units. J Stat Comput Sim 92(1):81–100. https://doi.org/10.1080/00949655.2021.1931212

West PW, Ratkowsky DA, Davis AW (1984) Problems of hypothesis testing of regressions with multiple measurements from individual sampling units. For Ecol Manag 7(3):207–224. https://doi.org/10.1016/0378-1127(84)90068-9

Yue C, Kohnle U, Kahle HP, Klädtke J (2012) Exploiting irregular measurement intervals for the analysis of growth trends of stand basal area increments: a composite model approach. For Ecol Manag 263:216–228. https://doi.org/10.1016/j.foreco.2011.09.007

Zeide B (1993) Analysis of growth equations. For Sci 39(3):594–616. https://doi.org/10.1093/forestscience/39.3.594

Zellner A (1962) An efficient method of estimating seemingly unrelated regressions and tests for aggregation bias. J Am Stat Assoc 55(298):348–368. https://doi.org/10.1080/01621459.1962.10480664

Zellner A (1963) Estimators for seemingly unrelated regression equations: some exact finite sample results. J Am Stat Assoc 58(304):977–992. https://doi.org/10.1080/01621459.1963.10480681

Zhang LJ, Bi HQ, Gove JH, Heath LS (2005) A comparison of alternative methods for estimating the self-thinning boundary line. Can J for Res 35(6):1507–1514. https://doi.org/10.1139/X05-070

Zhang XQ, Chhin S, Fu LY, Lu LL, Duan AG, Zhang JG (2019) Climate-sensitive tree height-diameter allometry for Chinese fir in southern China. Forestry 92(2):167. https://doi.org/10.1093/forestry/cpy043

Publisher's Note Springer Nature remains neutral with regard to jurisdictional claims in published maps and institutional affiliations.